

## Adsorption isotherms, kinetics and thermodynamic studies of methylene blue dye removal using *Raphia taedigera* seed activated carbon

Emmanuel F. Olasehinde<sup>1</sup>, Segun M. Abegunde<sup>2\*</sup>, Matthew A. Adebayo<sup>1</sup>

1. Department of Chemistry, Federal University of Technology, Akure, Ondo State, Nigeria

2. Department of Science Technology, Federal Polytechnic, Ado-Ekiti, Ekiti State, Nigeria

\*Corresponding author's email: abegundes@gmail.com

### ABSTRACT

This present work revealed the isotherm, kinetic, and thermodynamic behaviour of methylene blue (MB) dye adsorbed onto acidic activated carbon (AAC) and base activated carbon (BAC) prepared from *Raphia taedigera* seed by carbonization and chemical activation. AAC and BAC were activated with sulphuric acid and sodium hydroxide respectively. Batch equilibrium studies were done under different experimental conditions such as MB dye concentration and temperature. The equilibrium data were modelled using Langmuir, Freundlich, Elovich, Temkin and Dubinin-Radushkevich isotherms. The Langmuir isotherm model best describes the uptake of MB dye onto AAC and BAC with  $R^2 > 0.998$  in all cases. The pseudo-first-order, pseudo-second-order and intra-particle diffusion equations were used to evaluate the kinetic properties. It was observed that the adsorption of MB dye onto the two activated carbons could best be described by the pseudo-second order equation with  $0.999 < R^2 \leq 1$ . Thermodynamic parameters such as Gibbs free energy ( $\Delta G^0$ ), standard enthalpy ( $\Delta H^0$ ), standard entropy ( $\Delta S^0$ ), and activation energy ( $E_a$ ) were determined. The results of  $\Delta G^0$  indicated a spontaneous and feasible for AAC and non-spontaneous but feasible for BAC. Results of  $\Delta H^0$  confirmed that the adsorption of MB onto AAC and BAC are endothermic and physical in nature. It can be concluded that AAC and BAC prepared from *Raphia taedigera* seed could be used as low-cost adsorbent for the removal of MB dye from the wastewater.

**Key words:** *Raphia taedigera*; activated carbon; Langmuir; kinetic; methylene blue.

### INTRODUCTION

Textile effluents constitute most undesirable and major world's environmental problems. Textile industries consume a lot dyes and produce large amounts of wastewater, containing several contaminants. It is reported that 15% of about  $7 \times 10^5$  metric tonnes of over 10,000 commercially available dyes produced yearly are lost in textile wastewater during production and processing operation (Auta & Hameed 2011; Gupta *et al.* 2012; Gouamid *et al.* 2013; Deepak *et al.* 2017). The contaminants include acidic or caustic dissolved solids, heavy metals, toxic compounds, and dyes (Ahmad *et al.* 2014). The indiscriminate and continuous release of textile effluents is currently a major concern from a global viewpoint. The discharged dye waste into water streams poses a potential risk to aquatic environment due to bioaccumulation (Gouamid *et al.* 2013). Inhalation of methylene blue dye causes short periods of rapid or difficult breathing; ingestion through the mouth causes a burning sensation and may cause vomiting, nausea, gastritis, and diarrhoea. A large dose of methylene blue dye creates chest and abdominal pain, severe headache, mental confusion, profuse sweating, and methemoglobinemia-like syndromes (Bhattacharyya & Sharma 2005). Owing to wider applications of dye materials and their many hazards and toxic derivatives, the need for treatment of dye effluent becomes environmentally important (Ghaedi *et al.* 2013).

Several physical, chemical and biological methods have been employed, including coagulation/flocculation, adsorption, oxidation, membrane filtration and ozonation for the treatment of dye effluent. The characteristic features of various techniques have been extensively reviewed and reported (Hameed 2009; Deepak *et al.* 2017). However, most conventional methods have many disadvantages, including less efficiency, expensive, high cost of reagents and energy requirement. An alternative technique is the adsorption method using agriculture waste which is the focus of many scientists. The main advantages of this method can be considered as low initial cost, environmentally friendly, simple and short operating time compared to other conventional methods (Kismir & Aroguz 2011; Boldizar *et al.* 2017; Aseel *et al.* 2017).

For adsorption technique, the use of agricultural waste products appears to give a reliable prospect for dye removal. Hence, many researches, over the decade have focused on the use of agricultural waste product such as groundnut thull, banana stalk, oil palm fruit fibre, rice husks, mango peels, cocoa pod husks (Yahaya *et al.* 2010; Bello *et al.* 2012a; Bello *et al.* 2012b; Bello 2013) have been used for the dye removal from aqueous solution. Performance optimization of adsorption capacity has a direct relationship with reaction conditions: temperature, contact time, reaction pH, adsorbate concentration and adsorbent dosage. Temperature is an important parameter in adsorption technique (Michael & Ayebaemi 2015). The adsorbent-adsorbate behaviour with changes in temperature provides vital information in material development and applications. Data obtained during the evaluation of different adsorption conditions, including temperature are employed in adsorption modelling. Adsorption modelling (isotherms, kinetics and thermodynamic studies) provides vital information for research and design of new technique as well as predicting and evaluating changes in operating conditions of chemical processes.

*Raphia taedigera* belongs to the family of Arecaceae and grows in swamp forest along streams. It is native to Brazil, Nigeria, Costa Rica, Cameroon, Panama, and Nicaragua (Abegunde 2018). It produces fruit of about 5 – 7 cm long and 3 – 4 cm in diameter that are covered by imbricate glossy reddish-brown scales. The fruit, containing an egg-size single seed, is hard when dried with brown outer part and white shiny inner (Olasehinde & Abegunde 2019). In this work, equilibrium data were analysed using different equilibrium isotherm models. Kinetic data were modelled by pseudo-first order, pseudo-second order, Intra-particle diffusion and Elovich models. Thermodynamic parameters such as free Gibbs energy ( $\Delta G$ ), the change in enthalpy ( $\Delta H$ ) and entropy ( $\Delta S$ ) were also evaluated to understand the spontaneity of the adsorption process.

## MATERIALS AND METHODS

### Preparation of Activated Carbon

*Raphia taedigera* seeds were obtained locally from a farmland in Ado-Ekiti, Nigeria. The seeds were separated from debris, washed with distilled water and sun dried for several days and crushed. 100 g of the crushed *R. taedigera* seed was carbonized in a muffle furnace at 350°C for about 2 hours. The carbonized sample was cooled, washed with distilled water to attain the pH of 7 and dried at 105°C in an oven to constant weight. Chemical activation was done using sulphuric acid and sodium hydroxide solution. Activation was done as reported by Bello *et al.* (2017). 20 g of carbonized seed was weighed and transferred quantitatively into a clean 500 mL beaker. 200 mL 0.1 M sulphuric acid solution was added and agitated at 150-rpm for one hour and allowed to stand for about 24 hours. The activating agent, sulphuric acid was washed off the impregnated material with distilled water until pH 7.0. The activated material was transferred into an oven and dried at 105°C to constant weight. The dried material was sieved to obtain a fine powder of acidic *R. taedigera* activated carbon (AAC) and stored in an airtight plastic container for further use. The above – mentioned activation process was repeated using 0.1 M sodium hydroxide solution to produce base activated carbon (BAC). All reagents used were of analytical grade. All solutions were prepared with double distilled water.

### Preparation of dye solution (adsorbate)

0.1 g methylene blue ( $C_{16}H_{18}N_3SCl \cdot 3H_2O$ ) dye was weighed and dissolved in distilled water in a 250 mL beaker. This was then transferred into a volumetric flask of 1,000 mL capacity and made up to the mark with distilled water. This gave 100 mg L<sup>-1</sup> methylene blue (MB) and was labelled appropriately as a stock solution.

### Batch Adsorption Studies

Batch adsorption studies were carried out by shaking 0.50 g of activated carbons (AAC and BAC) separately with 10 mL of 100 mg L<sup>-1</sup> methylene blue (MB) in a 125 mL Erlenmeyer flask. The pH of the solution was adjusted using 0.1 M HCl or 0.1 M NaOH solution to 7. The flask was agitated at 150-rpm for 25 min to ensure equilibrium was reached. The resulting MB solution was separated from the sorbent by Whatman No 42 filter paper and the filtrate was stored in the sample bottle. The concentration of methylene blue in the filtrate was determined by UV-1800 series spectrophotometer using the wavelength obtained from sample scanning. The above experiment (at 298 K) was repeated at 308 K and 318 K. The uptake values were determined as the difference between the initial MB concentration and that of the resulted solution. The amount of MB adsorbed per unit mass of the adsorbent was calculated using Equation 1:

$$q_e = \frac{(C_0 - C_e)V}{W} \quad (1)$$

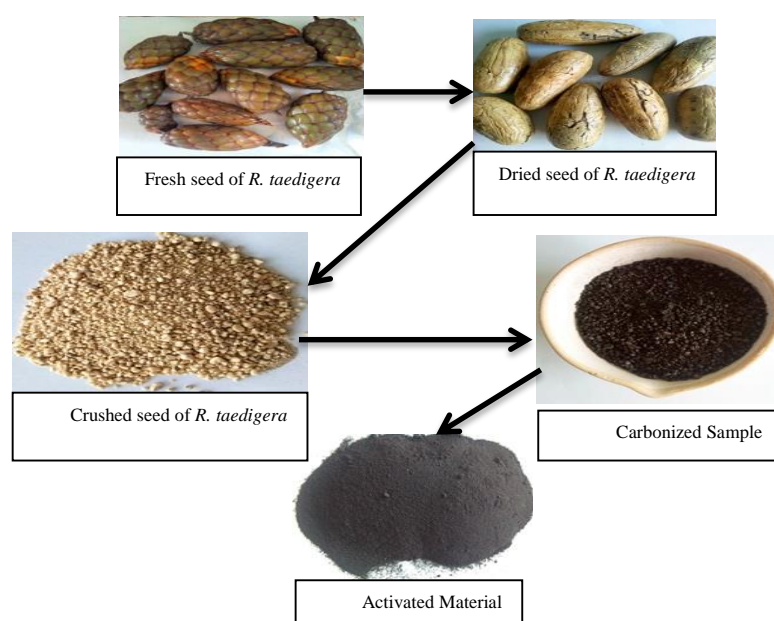


**Fig. 1.** Steps for the preparation of activated carbons.

where,  $q_e$  is the amount of MB adsorbed per unit mass in mg g<sup>-1</sup>,  $C_0$  is the initial MB concentration in mg L<sup>-1</sup>,  $C_e$  is the MB concentration at equilibrium in mg L<sup>-1</sup>,  $V$  is the volume of MB solution in mL and  $W$  is the mass of the adsorbent in grams.

The adsorption efficiency or MB removal rate (%) was calculated using the Equation 2

$$\text{Adsorption efficiency} = \frac{C_0 - C_e}{C_0} \times 100 \quad (2)$$

### Adsorption Isotherm

Adsorption isotherms predict the relationship between adsorbent and adsorbate (Mittal *et al.*, 2010). Isotherms explain how adsorbing materials interact with pollutants and hence, they are important in optimizing the use of adsorbents. Langmuir isotherm model assumes that adsorption takes place on a homogeneous surface and that it can only occur on a fixed active site and also can only hold one adsorbate molecule at a time (monolayer) without interaction between adsorbed molecules. The Langmuir adsorption isotherm can be represented by Equation 3 (Langmuir 1916).

$$\frac{C_e}{q_e} = \frac{1}{K_L q_m} + \frac{C_e}{q_m} \quad (3)$$

The shape of this isotherm can also be expressed in terms of separation factor ( $R_L$ ), which is given as (Foo, 2012):

$$R_L = \frac{1}{1 + K_L C_0} \quad (4)$$

where,  $q_e$  is the amount of MB adsorbed per unit mass in  $\text{mg g}^{-1}$ ,  $C_e$  is the MB concentration at equilibrium in  $\text{mg L}^{-1}$ ,  $q_m$  is the maximum amount of adsorbate adsorbed per unit weight of adsorbent,  $K_L$  ( $\text{L/mg}$ ) is Langmuir constant and  $C_0$  is the initial MB concentration in  $\text{mg L}^{-1}$ . The  $R_L$  value determines the shape of the isotherm to be unfavourable ( $R_L > 1$ ), linear ( $R_L = 1$ ), favourable ( $0 < R_L < 1$ ), or irreversible ( $R_L = 0$ ).  $R_L$  is defined by the following equation:

### Freundlich Isotherm Model

Freundlich isotherm assumes that adsorption takes place on a heterogeneous surface with a non-uniform distribution of heat of adsorption through a multilayer adsorption mechanism. The Freundlich isotherm can be expressed by the following equation (Olasehinde *et al.* 2018):

$$q_e = K_F C_e^{1/n} \quad (5)$$

The linearized form of Equation 5 is given as:

$$\log q_e = \log K + \frac{1}{n} \log C_e \quad (6)$$

where  $q_e$  is the amount of MB adsorbed per unit mass,  $C_e$  is the MB concentration at equilibrium,  $K_F$  and  $n$  are Freundlich constants.

### Elovich isotherm model

The assumption of an Elovich isotherm model is based on kinetic principle. It assumes that the sites for adsorption increase exponentially with adsorption, which implies a multilayer adsorption. The Elovich equation which was presented in 1939 is satisfied in chemisorption and is suitable for heterogeneous adsorbing surface systems (Aharoni, and Tompkins, 1970). The Elovich isotherm model isotherm is expressed as given in equation below:

$$\ln \frac{q_e}{C_e} = \ln K_E q_m - \frac{1}{q_m} q_e \quad (7)$$

where  $q_m$  ( $\text{mg g}^{-1}$ ) is the Elovich maximum adsorption capacity,  $C_e$  is the MB concentration at equilibrium,  $K_E$  is the Elovich equilibrium constant.

### Temkin isotherm model

The Temkin isotherm model takes into account the impact of indirect adsorbate-adsorbing species interactions on adsorption. It predicts that the heat of adsorption as a function of temperature of all the molecules in the layer would decrease linearly rather than logarithmically with coverage due to interactions adsorbent and adsorbate (Tempkin & Pyzhev 1940). It also assumes a uniform distribution of binding energies over a number of exchange sites on the surface. The Temkin isotherm model is expressed as:

$$q_e = B \ln K_T + B \ln C_e \quad (8)$$

where  $B$  is Temkin constant related to the heat of adsorption measured in  $\text{kJ mol}^{-1}$ , and  $A_T$  is the empirical Temkin constant which denotes the equilibrium binding constant related to the maximum binding energy ( $\text{L mg}^{-1}$ ).

### Dubinin-Radushkevich Isotherm model

The Dubinin-Radushkevich (D-R) isotherm model assumes that adsorption has a multilayer character, involves van der Waals forces indicating physical adsorption processes. The D-R isotherm model is a semi-empirical

equation where adsorption follows a pore filling mechanism. The Dubinin-Radushkevich isotherm model is expressed as given in equation below (Olasehinde *et al.* 2018):

$$\ln q_e = \ln q_m - K_{ad}\mathcal{E}^2 \quad (9)$$

where  $\mathcal{E}$  is given as:

$$\mathcal{E} = RT \ln(1 + 1/C_e) \text{ is Polanyi potential} \quad (10)$$

where,  $q_e$  is the amount of MB adsorbed per unit mass in  $\text{mg g}^{-1}$ ,  $q_m$  is the maximum amount of adsorbate adsorbed per unit weight of adsorbent, and  $K_{ad}$  ( $\text{mol}^2 \text{kJ}^{-2}$ ) is the constant related to sorption energy. The mean free energy of adsorption ( $E$ ) defined as the free energy change when 1 mole of ion is transferred to the surface of the adsorbent from infinity in solution can be evaluated from the  $\mathcal{E}$  value obtained.

$$E = 1/\sqrt{2}k_{ad} \quad (11)$$

If the magnitude of  $E$  is between 8 to 16  $\text{kJ mol}^{-1}$ , then the sorption process is supposed to proceed via chemisorption reaction, while for values of  $E < 8 \text{ kJ mol}^{-1}$ , the sorption process is physical in nature (Kundu & Gupta 2016).

### Adsorption Kinetics

In order to have a quantitative understandings of adsorption mechanism, kinetic models can be employed.

#### Pseudo-first order kinetic model

The pseudo-first-order kinetic model assumes that the rate of adsorption on adsorbent is proportional to the number of available active sites on the adsorbent. The rate constant for the adsorption for this present study for determining from a linearized form of pseudo-first order rate equation as stated below (Senthilkumaar 2005):

$$\log(q_{eq} - q_t) = \log(q_{eq} - \frac{k_1 t}{2.303}) \quad (12)$$

where  $q_{eq}$  is the amount of MB adsorbed at equilibrium ( $\text{mg g}^{-1}$ ),  $q_t$  is the amount of MB adsorbed at time  $t$  ( $\text{mg g}^{-1}$ );  $k_1$  is the equilibrium rate constant of pseudo-first sorption ( $\text{min}^{-1}$ ).

The first kinetic model is the generalised first-order kinetic equation proposed by Annadurai and Krishnan (Annadurai and Krishnan, 1996).

$$\frac{1}{q_t} = \frac{k_1}{q_e} \cdot \frac{1}{t} + \frac{1}{q_e} \quad (13)$$

#### Pseudo-second-order kinetic model

The pseudo-second-order kinetic model assumes that the rate limiting step may be chemical sorption involving valence forces through the sharing or exchange of electron between the methylene blue molecule and adsorbent. According to the pseudo-second order kinetic model, the rate of adsorption reaction decreases non-linearly with time. The pseudo-second order linearized equation is expressed as in equation 14 stated below (Ahmad *et al.* 2014):

$$\frac{t}{q_t} = \frac{1}{k_2 q_e^2} + \frac{1}{q_e t} \quad (14)$$

where,  $q_t$  is the amount of MB adsorbed at time  $t$  ( $\text{mg g}^{-1}$ );  $k_2$  is the equilibrium rate constant for the pseudo-second-order adsorption ( $\text{g/mg/min}$ ).

### Weber and Morris intra-particle diffusion kinetic model

Weber and Morris intra-particle diffusion kinetic model is the type of the diffusion model involved in adsorption processes expressed as Olasehinde *et al.* (2018):

where  $k_{id}$  ( $\text{mg/g s}^{1/2}$ ) is the intra-particle rate constant and  $C$  give an idea about the boundary layer thickness that is the intercept; the greater intercept; the greater is the boundary layer effect.

$$q_t = k_{id}t^{1/2} + C \quad (15)$$

where,  $k_{id}$  ( $\text{mg/g s}^{1/2}$ ) is the intra-particle diffusion rate constant. According to Eq. 15, a plot of  $q_t$  versus  $t^{1/2}$  should be a straight line with a slope  $k_{id}$  and intercept  $C$  which gives an idea about the boundary layer thickness, i.e. the larger the intercept, the greater the boundary layer effect. The linear plot of  $q_t$  versus  $t^{1/2}$  with zero intercept indicates that intra-particle alone determines the overall rate of adsorption.

### Thermodynamic studies

Thermodynamic parameters such as Gibbs free energy change ( $\Delta G$ ), enthalpy change ( $\Delta H$ ) and entropy change ( $\Delta S$ ) provide a better understanding of the temperature effect on the adsorption process. The obtained experimental data from batch adsorption experimental were analysed using the following thermodynamic equations:

$$K_c = \frac{C_s}{C_e} \quad (16)$$

where,  $C_s$  is the MB concentration on the adsorbent at equilibrium in  $\text{mg L}^{-1}$ ,  $C_e$  is the equilibrium concentration of the MB in a solution in  $\text{mg L}^{-1}$  and  $K_c$  is the thermodynamic equilibrium constant. The Gibbs free energy,  $\Delta G^0$  ( $\text{kJ mol}^{-1}$ ) for the adsorption MB onto the adsorbents can be calculated as follows:

$$\Delta G^0 = -RT \ln \quad (17)$$

where  $T$  is the absolute temperature (K) and  $R$  is the universal gas constant ( $8.314 \text{ J/mol/k}$ ). Enthalpy and entropy are obtained using Van't Hoff's equation (Deepak *et al.* 2017). The change in free energy is related to other thermodynamic properties as:

$$\Delta G^0 = \Delta H^0 - T\Delta S^0 \quad (18)$$

$$\ln K_c = \Delta S^0/R - \Delta H^0/RT \quad (19)$$

where  $T$  is the absolute temperature (K) and  $R$  is the universal gas constant ( $8.314 \text{ J/mol/k}$ ),  $\Delta H^0$  is the change in enthalpy and  $\Delta S^0$  is the degree of disorderliness of a reaction.  $\Delta H^0$  and  $\Delta S^0$  can be obtained from the plot of  $\ln K_c$  against  $1/T$ .

## RESULTS AND DISCUSSION

### Effect of time

The effect of temperature on the removal of MB was investigated. The results were presented in Fig. 2. Based on the Fig. the adsorption of MB onto the activated carbons has been observed to increase by upraising temperature from 25 to 45°C. The increase in the adsorption capacity of AAC and BAC with temperature indicates endothermic

adsorption process. It can be inferred that the increased adsorption by rising in temperature was due to an elevation in the number of active surface sites available for adsorption on the adsorbents.

### Adsorption isotherm

Adsorption isotherms explain how adsorbent materials interact with pollutants and hence, they are important in optimizing the use of bio-sorbents. Determination of equilibrium parameters provides important information for the design of adsorption system dye removal from solutions (Witek-Krowiak *et al.* 2011), it is therefore necessary to establish the most appropriate correlation for the equilibrium curve. The model isotherms employed in this study include Langmuir, Freundlich, Elovich, Temkin, and Dubinin-Radushkevich (D-R) adsorption isotherms. The Langmuir adsorption isotherm linearized form was given in Equation 3. Plots of  $C_e/q_e$  against  $C_e$  for the adsorption of methylene blue onto AAC and BAC are presented in Figs. 3 and 4, respectively. The values of  $q_{max}$  and  $K_L$  ( $L\ mg^{-1}$ ) are Langmuir parameters obtained from the slope and intercept of the plot of  $C_e/q_e$  against  $C_e$  respectively and correlation coefficient ( $R^2$ ) are presented in Table 1. As shown in the table, the correlation coefficients ( $R^2$ ) are all greater than 0.998 at all temperatures indicating strong relationship between the adsorption data. Increase in  $K_L$  values as temperatures increased implies that a stronger adsorption taking place (Wang *et al.* 2017). Values of  $q_{max}$  for both AAC and BAC elevated by raised temperature suggesting endothermic reactions. This could be as a result of the increased rate of diffusion of the molecules while declining in the viscosity of liquid at higher temperature, which facilitates easier migration of adsorbate molecules towards and through adsorbents pores. To establish whether the adsorption process is favourable or not, a dimensionless constant known as a separation factor ( $R_L$ ) is evaluated as defined in Equation 4. The values are  $1 > R_L > 0$  at all working temperatures, indicating that the adsorption processes are favourable.

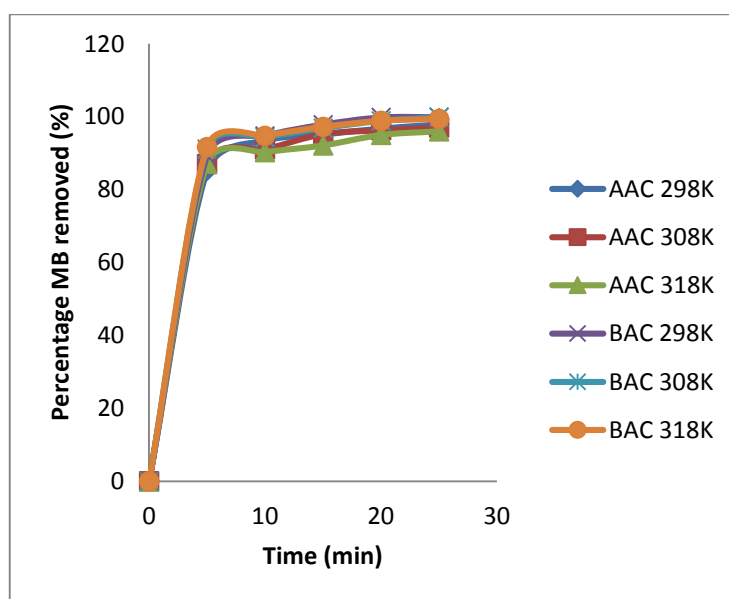


Fig. 2. Plots of percentage removal against time.

The linearized form of Freundlich isotherm model was expressed in Equation 6. The plots of  $\log q_e$  against  $\log C_e$  for the adsorption of MB onto AAC and BAC are presented in Figs. 5 and 6, respectively. Table 1 presents  $k_F$  and  $n$  values obtained from the intercepts and slopes of  $\log q_e$  versus  $\log C_e$ . The slope, ( $1/n$ ), ranging from 0 to 1 is a measure of intensity of adsorption or surface heterogeneity. The surface becomes more heterogeneous as the value  $1/n$  approaches zero, while a value of  $1/n$  below 1 indicates a normal Langmuir isotherm while a value of  $1/n$  above 1 is indicative of cooperative adsorption (Fytianos *et al.* 2000; Rauf 2008). The correlation coefficients at all temperatures for AAC and BAC are close to unity, thus indicating that the data can be represented by Freundlich isotherm model. It is also important to note from Table 1 that the values of  $n$  are greater than 1 at all the temperatures for both activated carbons, and the values of  $1/n$  increased slightly by upraised temperature while the value of  $n$  dropped by the temperature upraising. The values of  $n$  greater than unity indicated a favourable adsorption taking place, while the values of  $1/n$  tending towards zero revealed the heterogeneity of

the surface. The values of  $K_F$  which is an indication of adsorption capacity increased slightly at higher temperature, implying an increased temperature is beneficial to the process. The Elovich isotherm model isotherm was expressed as given in Equation 7. The Plots of  $\ln q_e/C_e$  against  $q_e$  for the adsorption of MB onto AAC and BAC are presented in Figs. 7 and 8, respectively. The values of  $K_E$  and  $q_e$  were obtained from the intercept and the slope of the plot, and presented in Table 1. In all cases, the Elovich isotherm can be said to exhibit high value of correlation coefficients. However, the maximum adsorption capacity ( $q_e$ ) values determined from the linear plots of Elovich equation, and contained in Table 1 are much lower than the experimental amount of MB adsorbed at equilibrium corresponding to the peaks of the adsorption isotherms despite the good correlation coefficients. This means multilayer adsorption is not in conformance with the experiment within the studied concentration. Hence, the Elovich model is not enough to explain the adsorption isotherms of MB onto the materials. The Temkin isotherm model was stated in Equation 8. Plots of  $q_e$  versus  $\ln C_e$  are presented in Figs. 9 and 10 for AAC and BAC, respectively enabling the determinations of the isotherm constants  $A_T$  and  $B$  from the intercept and slope of the curves respectively. The processes were exothermic as indicated by negative energy values (Inam *et al.*, 2017). It was also observed from Table 1 that the values of  $B_T$  are all less than  $8 \text{ kJ mol}^{-1}$ , indicating that the interaction between the adsorbent and adsorbate are weak, thus, the adsorption mechanism put into play here is merely that of an ion exchange (Ghogomu *et al.* 2013). The Dubinin-Radushkevich isotherm model was expressed in Equation 9. The plots of  $\ln q_e$  against  $\mathcal{E}^2$  were presented in Figs. 11 and 12 for the adsorption of MB onto AAC and BAC, respectively. The D-R constant related to sorption energy,  $K_{ad}$ , measured in  $\text{mol}^2 \text{ KJ}^{-2}$  and the amount of sorbate adsorbed by sorbent,  $q_{max}$ , in  $\text{mol g}^{-1}$  were obtained from the slope and intercept of the plots respectively and presented in Table 1. The mean free energy of adsorption ( $E$ ) was also calculated from  $\epsilon$  values using Eq. 11 and the values were presented in Table 1. According to this table, the values of the adsorption energy at all temperatures for the two ACs is less than  $8 \text{ kJ mol}^{-1}$ , thereby it can be concluded that the adsorption processes were dominated by physical forces. Noteworthy, the value of  $R^2$  in all cases is lower than those obtained with other adsorption isotherms, indicating that adsorption of MB onto the two adsorbent does not fit the Dubinin-Radushkevich Isotherm model.

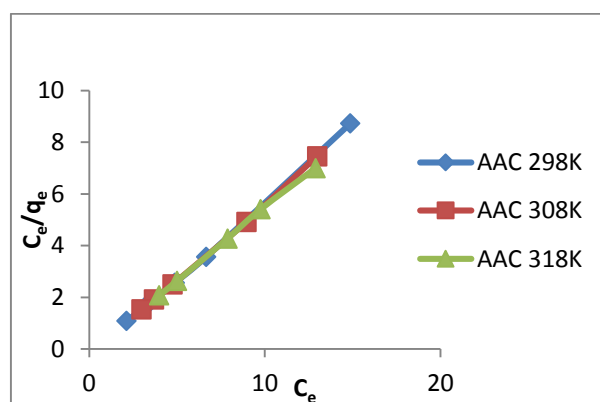


Fig. 3. Langmuir isotherm plot for AAC.

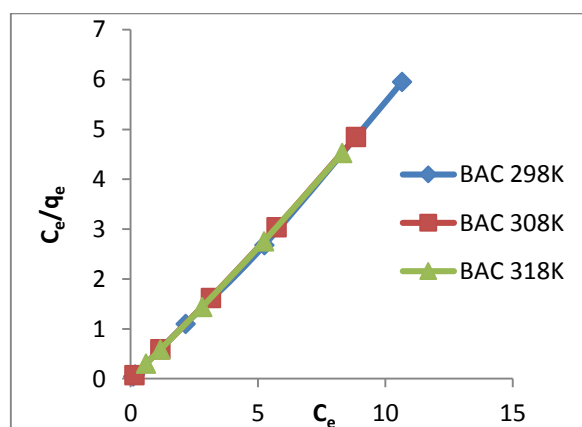


Fig. 4. Langmuir isotherm plot for BAC.

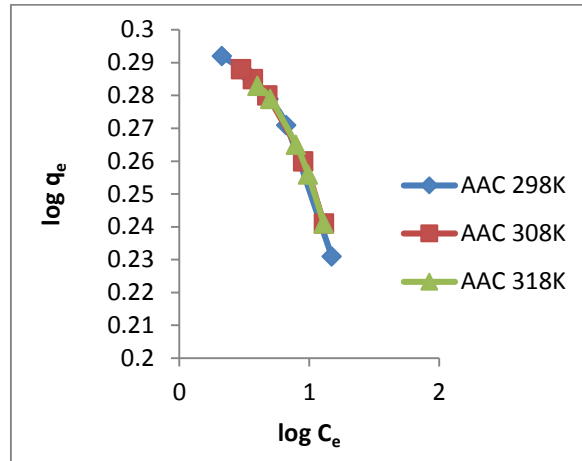


Fig. 5. Freundlich Adsorption isotherm AAC.

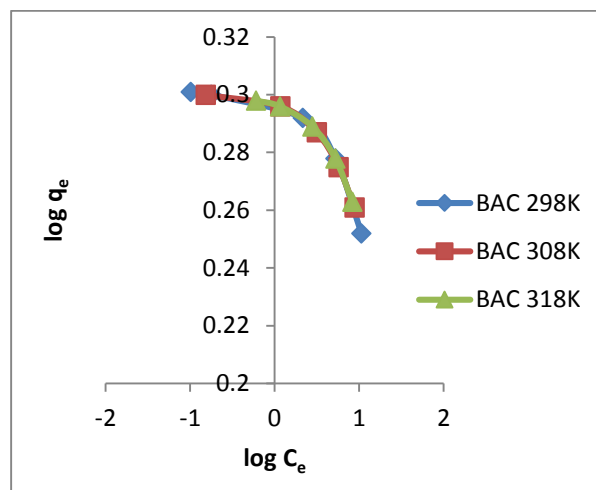


Fig. 6. Freundlich Adsorption isotherm BAC.

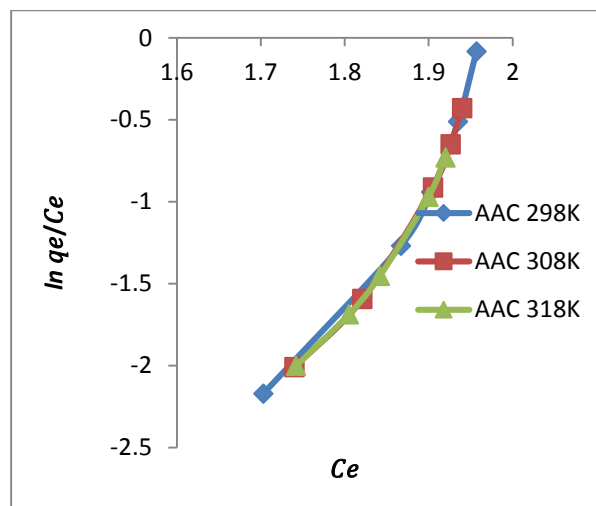


Fig. 7. Elovich Adsorption isotherm of AAC.

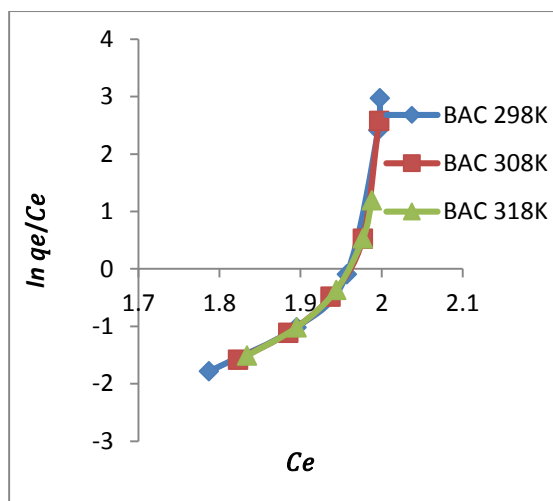


Fig. 8. Elovich Adsorption isotherm of BAC.

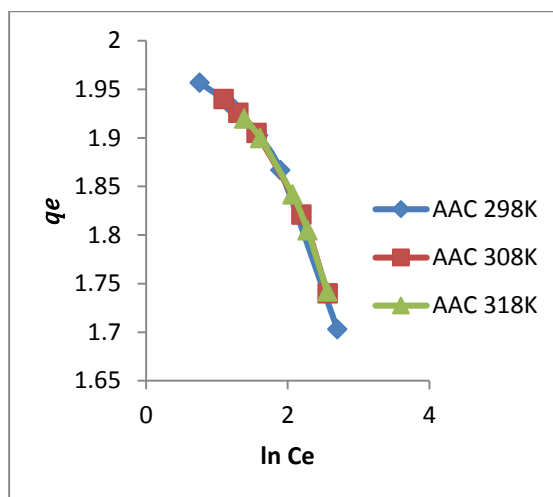


Fig. 9. Temkin Adsorption isotherm AAC.

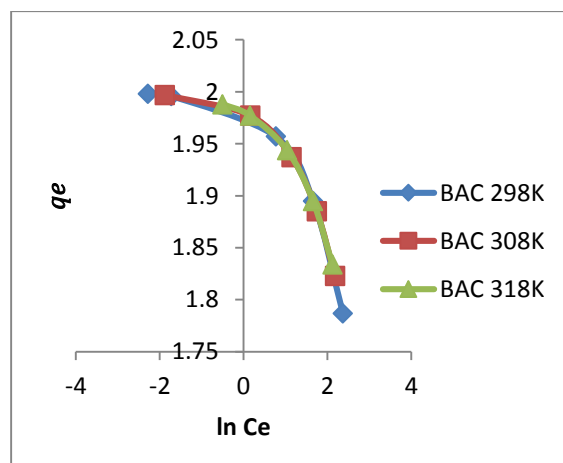


Fig. 10. Temkin Adsorption isotherm BAC.

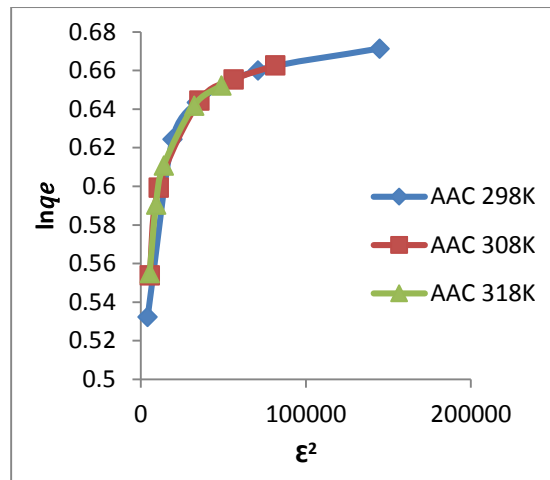


Fig. 11. Dubinin-Radushkevich (D-R) Isotherm for AAC.

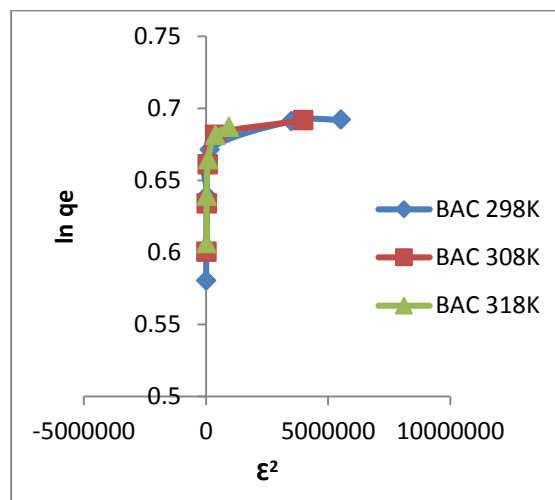


Fig. 12. Dubinin-Radushkevich (D-R) Isotherm for BAC.

### Adsorption Kinetics

To investigate the mechanism of adsorption of MB onto AAC and BAC, the potential rate determining step, such as mass transport and chemical reactions, pseudo-first-order, pseudo-second-order and diffusion-based kinetic models were used to simulate the experimental data. These empirical mathematical models which describe laboratory batch adsorption data are proven useful as tools to scale up process optimization (Senthikumaar *et al.* 2010). The linearized form of pseudo-first-order kinetic model was expressed in Equation 13. A plot of  $1/q_t$  against  $1/t$  is presented in Fig. 13 from which the values of the pseudo-first-order parameters  $q_e$ ,  $k_1$  and  $R^2$  were obtained and reported in Table 2. Based on these data, though  $R^2$  values were high, however, the calculated values of  $q_e$  were far below the corresponding experimental values; hence, pseudo-first order kinetic model was not proved to be the best fit in representing the experimental kinetic data for the concentration under study at all temperatures. The pseudo-second order linearized equation was stated in Equation 14. A plot of  $t/q_t$  against  $t$  is presented in Fig. 14. The pseudo-second-order parameters  $q_e$ ,  $k_2$  and  $R^2$  were calculated for the adsorption of MB onto the ACs and presented in Table 2. The values of  $q_e$  and  $k_2$  were obtained from the intercept and slope of plot in Fig. 14 respectively. As shown in the table, the values of correlation coefficient at all temperatures is greater than 0.999 with  $R^2 = 1$  (unity) at 298 K for AAC. The Weber and Morris intra-particle diffusion kinetic model equation is expressed as in Equation 15. The linear plot of  $q_t$  versus  $t^{1/2}$  was presented in Fig. 17. The value of  $k_{id}$  was calculated from the slope in Fig. 15. The values  $C$  at all temperature are not equal to zero. This deviation from the origin was due to differences in the rate of mass transfer in the initial and final stages of adsorption. The results from a linear plot for adsorption of MB on AAC and BAC implies that the reaction cannot be represented by Weber and Morris intra-particle diffusion kinetic model. Comparing the data with those obtained with pseudo-first order kinetic model, it can easily be seen that the values of correlation coefficients are greater than 0.999 at

all temperatures and attained a correlation coefficient of 1 (unity) at 298 K for AAC. Also, the values of calculated adsorption capacity  $q_{e,cal}$  gave a better agreement with that of the experimental values  $q_{e,exp}$ . It can be said that adsorption processes follow pseudo-second order kinetic model for the concentration of the dye at all temperature. The results of similar findings have been reported for the adsorption of MB on AAC and BBC (Chiou 2004; Ofomaja & Ho 2007).

**Table 1.** Results of Adsorption Isotherm at temperature 298, 308 and 318 K.

Isotherms Equation	Parameters	RTA			RTB		
		298 K	308 K	318K	298 K	308 K	318 K
Langmuir $\frac{C_e}{q_e} = \frac{1}{KLq_m} + \frac{C_e}{q_m}$	$q_m$	1.6551	1.6906	1.7921	1.7973	1.8212	1.8245
	$K_L$	1.9216	2.1035	4.1035	8.5106	10.0402	9.0744
	$R_L$	0.0052	0.0047	0.0024	0.0012	0.000995	0.00110
	$R^2$	0.9988	0.9993	0.9992	0.9981	0.9994	0.9995
Freundlich $\log q_e = \log K_f + \frac{1}{n} \log C_e$	$1/n$	0.0723	0.0732	0.081	0.0198	0.0199	0.0290
	$n$	13.8312	13.6612	12.3457	50.5051	50.2513	34.4828
	$K_f$	2.1033	2.1193	2.1602	1.9315	1.9480	1.9770
Elovich $\ln \frac{q_e}{C_e} = \ln K q_m - \frac{1}{q_m} q_e$	$q_m$	0.1315	0.1291	0.1405	0.0476	0.0486	0.0606
	$K$	$3.14 \times 10^7$	$4.50 \times 10^7$	$1.37 \times 10^7$	$4.9 \times 10^{18}$	$3.33 \times 10^{18}$	$1.33 \times 10^{14}$
	$R^2$	0.9325	0.9738	0.9783	0.7830	0.7809	0.9011
Temkin $q_e = B \ln K_T + B \ln C_e$	$B$	-0.1309	-0.1346	-0.1483	-0.0378	-0.0385	-0.0561
	$K_T$	$8.3 \times 10^6$	$6.0 \times 10^6$	$1.8 \times 10^6$	$1.6 \times 10^{22}$	$9.8 \times 10^{21}$	$2.0 \times 10^{15}$
	$R^2$	0.9209	0.9695	0.9741	0.7742	0.7722	0.8952
Dubinin-Radushkevich $\ln q_e = \ln q_m - K_{ad} \epsilon^2$	$q_m$	1.7985	2.1908	1.8088	1.8793	1.900	1.8915
	$K_{ad}$	$7 \times 10^{-7}$	$1 \times 10^{-6}$	$2 \times 10^{-6}$	$1 \times 10^{-8}$	$1 \times 10^{-8}$	$6 \times 10^{-8}$
	$R^2$	0.5308	0.7845	0.7317	0.4925	0.3911	0.5555
	$E_a$	2.7020	0.7072	0.5000	7.0721	7.0721	4.0834

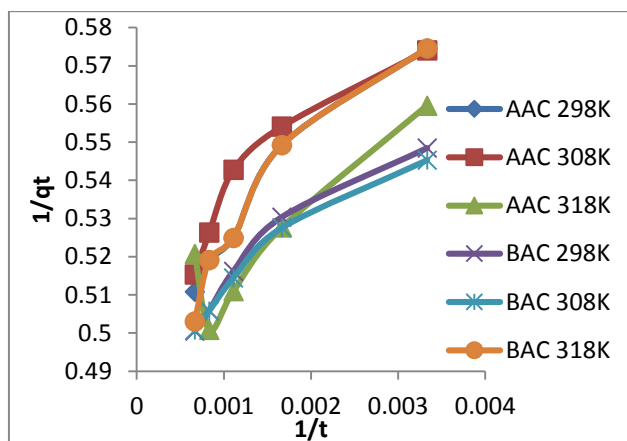


**Fig. 13.** Pseudo-first order equation.

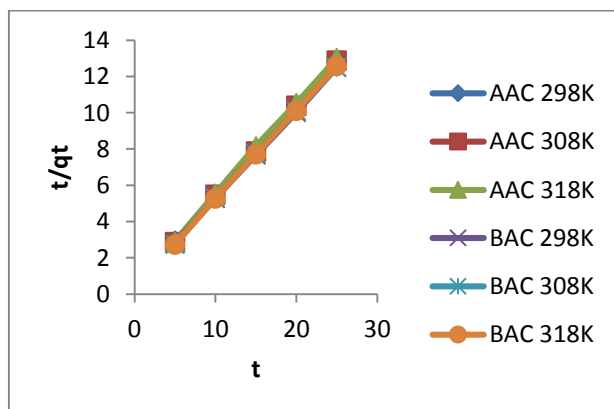


**Fig. 14.** Pseudo-second order equation.

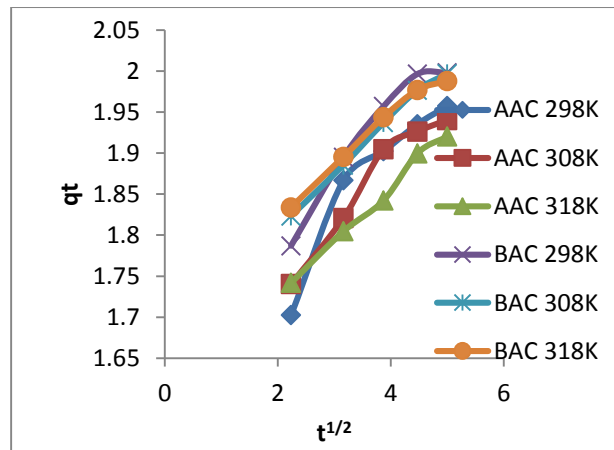


Fig. 15. Weber and Morris intra-particle diffusion model.

Table 2. Results of Adsorption Kinetics at temperature 298, 308 and 318 K.

Kinetic Model	Parameters	RTA			RTB		
		298 K	308 K	318 K	298 K	308 K	313 K
Pseudo-first-order $\frac{1}{qt} = \frac{K_1}{q_e t} + \frac{1}{q_e}$	$q_e$	0.0427	0.050	0.053	0.058	0.062	0.040
	$K_1$	0.021	0.026	0.026	0.029	0.031	0.020
	$R^2$	0.9483	0.8704	0.8502	0.9286	0.9414	0.9187
Pseudo- second-order $\frac{t}{qt} = \frac{1}{K_2 q_e^2} + \frac{1}{q_e} t$	$q_e$	2.028	2.006	1.977	2.069	2.052	2.037
	$K_2$	0.529	0.530	0.560	0.580	0.631	0.751
	$R^2$	1.0000	0.9998	0.9995	0.9999	0.9998	0.9999
Weber and Morris Intra-particle Diffusion Model $q_t = K_{diff} t^{1/2}$	$K_{id}$	0.0878	0.0646	0.0661	0.0788	0.0756	0.0578
	$C$	1.544	1.6317	1.5941	1.6312	1.5832	1.7110
	$R^2$	0.8908	0.9934	0.9912	0.9374	0.9495	0.9800

### Thermodynamic Studies

The values of the thermodynamic parameters such as change in free energy ( $\Delta G^0$ ), enthalpy ( $\Delta H^0$ ) and entropy ( $\Delta S^0$ ) were determined using Equations 16, 17, 18 and 19, presented in Table 3. The plot of  $\ln K_C$  as a function of  $1/T$  yields shown in Fig. 16 is a straight line from which enthalpy ( $\Delta H^0$ ) and entropy ( $\Delta S^0$ ) can be calculated from the slope and intercept, respectively. As shown in table 3, negative values were observed for  $\Delta G^0$  at all working temperatures for AAC and positive values for BAC. The negative values of  $\Delta G^0$  for the MB adsorption onto AAC exhibits that the adsorption processes were spontaneous and feasible. The positive values of  $\Delta G^0$  for the adsorption of MB onto BAC indicate that the reactions are feasible but non-spontaneous. The positive values of  $\Delta H^0$  confirmed that the adsorption of MB onto AAC and BAC are endothermic. Positive value of  $\Delta S^0$  observed for AAC reveals that the degree of disorderliness increased at the AACs-MB interface during the adsorption of MB onto AAC predicting low energy of attraction between the adsorbent and methylene blue molecules while the negative value of  $\Delta S^0$  observed for BAC displays that the degree of disorderliness is less at the BAC-MB interface than in the bulk solution. Also, the values of adsorption energy at all temperatures for both AAC and BAC are lower than  $8 \text{ kJ mol}^{-1}$ , therefore it can be concluded that the adsorption processes were dominated by physical forces.

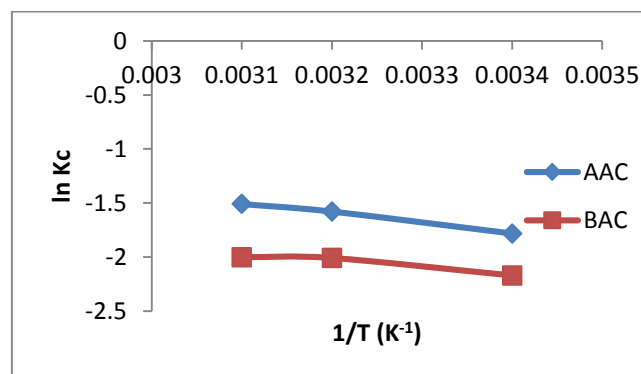


Fig. 16. Plot of  $\ln K$  against  $1/T$ .

**Table 3.** Results of Thermodynamic Studies.

Activated Carbon	Temperature	$\Delta G^0$ (KJ/mol)	$\Delta H^0$ (KJ/mol)	$\Delta S^0$ (J/mol/K)
AAC	298K	-3.42	+7.72	+11.47
	308K	-3.53		
	318K	-3.65		
BAC	298K	+0.31	+4.99	-1.01
	308K	+0.32		
	318K	+0.33		

## CONCLUSION

In this work, equilibrium, kinetic and thermodynamic studies were carried out on the adsorption of methylene blue onto AAC and BAC from aqueous solution. Langmuir, Freundlich, Elovich, Temkin and Dubinin-Radushkevich adsorption isotherm models were used to model the equilibrium data obtained from adsorption of methylene blue onto AAC and BAC. The equilibrium fitted best into Langmuir which indicated that the adsorption process occurred on homogeneous surface. The values of adsorption energy ( $E_a$ ) at all temperatures are lower than  $8 \text{ kJ mol}^{-1}$ , therefore it can be concluded that the adsorption processes were dominated by physical forces. The rate of adsorption was observed to follow pseudo-second order kinetics model with a good correlation coefficient. The  $\Delta G^0$  values confirmed that the adsorption of MB onto the AAC were spontaneous and feasible while adsorption through BAC were non-spontaneous but feasible. The positive  $\Delta H^0$  value indicated endothermic nature of adsorption of MB onto both AAC and BAC. It may be concluded that AAC and BAC prepared from *R. taedigera* seed may be used as low-cost for the removal of MB from the wastewater.

## REFERENCES

- Abegunde, SM, 2018, Proximate composition, phytochemical analysis and elemental characterization of *Raphia taedigera* seed. *Asian Journal of Chemical Sciences*, 5: 1-8.
- Aharoni, C & Tompkins FC, 1970, Kinetics of adsorption and desorption and the Elovich equation, in: DD Eley, H Pines & PB Weisz (Eds.), *Advances in catalysis and related subjects*. Vol. 21, Academic Press, New York, 1970, 1-49.
- Ahmad, MA, Puad, N & Bello, OS 2014, Kinetic, equilibrium and thermodynamic studies of synthetic dye removal using pomegranate peel activated carbon prepared by microwave-induced KOH activation. *Water Resources and Industry*, 6:18–35.
- Annadurai, G & Krishnan, MRV 1996, Adsorption of basic dye on chitin. *Indian Journal of Environmental Protection*, 16:444e9.
- Aseel, MA, Abbas, NA & Ayad, FA 2017, Kinetics and equilibrium study for the adsorption of textile dyes on coconut shell activated carbon, *Arabian Journal of Chemistry*, 10: S3381-S3393.
- Auta, M & Hameed, B 2011, Preparation of waste tea activated carbon using potassium acetate as an activating agent for adsorption of Acid Blue 25 dye. *Chemical Engineering Journal*, 171: 502-509.
- Ayawei, N, Ebelegi, AN & Wankasi, D 2017, Modelling and interpretation of adsorption isotherms. *Journal of Chemistry*, 1-11. DOI: <https://doi.org/10.1155/2017/3039817>
- Bello, OS, 2013, Adsorptive removal of malachite green with activated carbon prepared from oil palm fruit fibre by KOH activation and  $\text{CO}_2$  gasification, *South African Journal of Chemistry*, 66: 32-41.
- Bello, OS & Ahmad, MA 2011, Adsorption of dyes from aqueous solution using chemical activated mango peels. In: *Proceedings of the 2<sup>nd</sup> International Conference on Environmental Science and Technology (ICEST)*, 2: 108-113.
- Bello, OS, Fatona, TA, Falaye, FS, Osulale, OM & Njoku, VO 2012a, Adsorption of eosin dye from aqueous solution using groundnut hull based activated carbon: kinetic, equilibrium, and thermodynamic studies, *Environmental Engineering Science*, 29: 186-194.
- Bello, OS, Ahmad, MA & Ahmad, N 2012b, Adsorptive features of banana (*Musa paradisiaca*) stalk-based activated carbon for malachite green dye removal, *Chemical Ecology*, 28: 153–167.
- Bello, OS, Adegoke, KA & Akinyunni, OO 2017, Preparation and characterization of a novel adsorbent from *Moringa oleifera* leaf. *Applied Water Science*, 7: 12951305.
- Bhattacharyya, KG & Sharma, A 2005, Kinetics and thermodynamics of methylene blue adsorption on Neem (*Azadirachta indica*) leaf powder. *Dyes and Pigments*, 65: 51–59.

- Boldizar, N, Carmen, M, Andrada, M, Cerasella, I, Barbu-Tudoran, L & Cornelia, M 2017, Linear and nonlinear regression analysis for heavy metals removal using *Agaricus bisporus macrofungus*. *Arabian Journal of Chemistry*, 10: S3569-S3579.
- Brouers, F & Al-Musawi, TJ 2015, On the optimal use of isotherm models for the characterization of biosorption of lead onto algae. *Journal of Molecular Liquids*, 212: 46-51.
- Deepak, P, Shikha, S & Pardeep, S 2017, Removal of methylene blue by adsorption onto activated carbon developed from *Ficus carica bast*. *Arabian Journal of Chemistry*, 10, S1445-S1451.
- Foo, KY 2012, Preparation, characterization and evaluation of adsorptive properties of orange peel based activated carbon via microwave induced  $K_2CO_3$  activation. *Bioresource Technology*, 104, 679-686.
- Ghogomu, JN, Noufame, TD, Ketcha, MJ & Ndi, NJ 2013, Removal of Pb (II) ions from aqueous solutions by kaolinite and metakaolinite materials. *British Journal of Applied Science & Technology*, 3: 942-961.
- Gouamid, M, Ouahrani, MR & Bensaci, MB 2013, Adsorption equilibrium, kinetics and thermodynamics of methylene blue from aqueous solutions using date palm leaves. *Energy Procedia*, 36: 898-907.
- Gupta, VK, Pathania, D, Agarwal, S & Singh, P 2012, Adsorptional photocatalytic degradation of methylene blue onto pectin-CuS nanocomposite under solar light. *Journal of Hazardous Materials*, 243, 179-186.
- Hameed, BH 2009, Spent tea leaves: a new non-conventional and low-cost adsorbent for removal of basic dye from aqueous solutions. *Journal of Hazardous Materials*, 161: 753-759.
- Inam, E, Etim, UJ, Akpabio, EG & Umoren, SA 2017, Process optimization for the application of carbon from plantain peels in dye abstraction. *Journal of Taibah University for Science*, 11: 173-185.
- Kannan, N & Sundaram, MM 2001, Kinetics and mechanism of removal of methylene blue by adsorption on various carbons e a comparative study. *Dyes and Pigments*, 51: 25e40.
- Kismir, Y & Aroguz, AZ 2011, Adsorption characteristics of the hazardous dye brilliant green on Saklikent mud. *Chemical Engineering Journal* 172, 199-206.
- Kundu, S & Gupta, VK 2006, Arsenic adsorption onto iron oxide-coated cement (IOCC): Regression analysis of equilibrium data with several isotherm models and their optimization. *Chemical Engineering Journal*, 122: 93-106.
- Langmuir, I 1916, The constitution and fundamental properties of solids and liquids. *Journal of the American Chemical Society*, 38: 2221-2295.
- Michael, H & Ayebaemi, IS 2005, Effects of temperature on the sorption of  $Pb^{2+}$  and  $Cd^{2+}$  from aqueous solution by *Caladium bicolor* (Wild Cocoyam) biomass. *Electronic Journal of Biotechnology*, 8: 2.
- Mittal, A, Mittal, J, Malviya, A, Kaur & A, Gupta, VK 2010, Decoloration treatment of a hazardous triarylmethane dye, light green SF (yellowish) by waste material adsorbents. *Journal of colloid and interface science*, 342: 518-527
- Olasehinde, EF & Abegunde, SM 2020, Preparation and characterization of a new adsorbent from *Raphia taedigera* seed. *Research on Engineering Structure and Materials*, 6: 167-182.
- Olasehinde, EF, Adegunloye, AV, Adebayo, MA & Oshodi, AA 2018, Sequestration of aqueous lead (II) using modified and unmodified red onion skin, *Analytical Letters*, 51: 2710-2732.
- Salleh, MAM, Mahmoud, DK, Karim, WA & Idris, A 2011, Cationic and anionic dye adsorption by agricultural solid wastes: a comprehensive review. *Desalination*, 280: 1-13.
- Senthilkumaar, S, Varadarajan, PR, Porkodi, K & Subbhuraam, CV 2005, Adsorption of methylene blue onto jute fiber carbon: kinetics and equilibrium studies. *Journal of Colloid Interface Science*, 284: 78-82.
- Tempkin, MJ & Pyzhev, V 1940, Recent modification to Langmuir isotherms, *Acta Physicochimica*, USSR, 12: 217.
- Yahaya, NE, Pakir, MF, Latiff, M, Abustan, I, Bello, OS & Ahmad, MA 2010, Process optimization for Zn (II) removal by activated carbon prepared from rice husk using chemical activation, *International Journal of Engineering Technology*, 10:132-136.

## مطالعات جذب ایزوترم‌ها، کینتیکس و ترمودینامیک حذف متیلن بلو با استفاده از کربن فعال

### دانه *Raphia taedigera*

امانوئل ف. اولاسهینده<sup>۱</sup>، سگون م. آبگوندا<sup>۲\*</sup>، ماتيو ا. آدبايو<sup>۱</sup>

۱- گروه شیمی، دانشگاه فدرال تکنولوژی، آکوره، ایالت اوندو، نیجریه

۲- گروه فناوری علم، دانشگاه پلی تکنیک، آدو-اکیتی، ایالت اکیتی، نیجریه

(تاریخ دریافت: ۹۸/۱۰/۰۳ تاریخ پذیرش: ۹۹/۰۲/۱۱)

#### چکیده

مطالعه حاضر، رفتار ایزوترم، کینتیک و ترمودینامیک متیلن بلو جذب شده بر روی کربن فعال اسیدی و کربن فعال پایه تهیه شده از دانه رافیا تادیجرا توسط فعالیت کربن دار کردن و شیمیایی آشکار کرد. کربن فعال اسیدی و کربن فعال پایه به ترتیب توسط اسید سولفوریک و هیدروکسید سدیم صورت گرفت. مطالعات تعادلی batch در شرایط تجربی مختلف مانند غلظت متیلن بلو و دما انجام شد. مطالعات تعادلی با استفاده از ایزوترم Langmuir, Freundlich, Elovich, Temkin and Dubinin-Radushkevich مدل سازی شد. مدل ایزوترم لانگمویر به خوبی جذب متیلن بلو توسط کربن فعال اسیدی و کربن فعال پایه با  $R^2 > 0.998$  را توصیف کرد. معادلات شبه دستوری اولیه، ثانویه و انتشار درون ذره ای برای ارزیابی خواص کینتیک استفاده شد. مشاهده شد که جذب متیلن بلو بر روی دو کربن فعال را با معادله شبه دستوری ثانویه با  $0.999 < R^2 \leq 1$  بیش از دیگر معادلات می توان توصیف کرد. فراسنجه های ترمودینامیک مانند انرژی آزاد گیبس، استاندارد انتالپی، استاندارد آنتروپی و انرژی اکتیواسیون تعیین شدند. نتایج انرژی آزاد گیبس خودجوشی و امکان پذیر بودن جذب متیلن بلو بر روی کربن اسیدی اما غیر خودجوشی و البته امکانپذیری برای کربن پایه را نشان داد. نتایج استاندارد انتالپی نشان داد که جذب متیلن بلو توسط کربن فعال اسیدی و کربن فعال پایه ماهیت اندوترمیک و فیزیکی دارد. بنابر این می توان نتیجه گرفت که کربن فعال اسیدی و کربن فعال پایه رافیا تادیجرا را می توان به عنوان ماده جاذب ارزان قیمت برای جذب متیلن بلو استفاده کرد.

\*مؤلف مسئول

---

#### Bibliographic information of this paper for citing:

Olasehinde, E.F., Abegunde, S.M., Adebayo, M.A. 2020 Adsorption isotherms, kinetics and thermodynamic studies of methylene blue dye removal using *Raphia taedigera* seed activated carbon. Caspian Journal of Environmental Sciences, 18: 329-344

Copyright © 2020